STUDY OF TRANSVERSE AND DELAMINATION CRACKS IN [0/90] SYMMETRIC LAMINATES BY MEANS OF THE CLASSICAL LEFM AND THE LINEAR ELASTIC BRITTLE INTERFACE FORMULATION

L. Távara*[1], A. Blázquez[1], V. Mantič[1], E. Graciani[1], F. París[1]

[1] *Grupo de Elasticidad y Resistencia de Materiales, Escuela Técnica Superior de Ingeniería, Universidad de Sevilla, Camino de los Descubrimientos s/n, 41092 Seville, Spain*

* *ltavara@esi.us.es*

Keywords: Composites, delamination, mixed mode fracture, interface crack

Abstract

The onset and growth of transverse and delamination cracks in $[0/90]$ *symmetric laminates under traction loads in the fibre direction of the external laminas is studied. The problem is solved by means of the Boundary Element Method (BEM). Crack propagation is modeled by two different approaches. First, using the Virtual Crack Closure Technique (VCCT) to calculate the Energy Release Rate (ERR) in the framework of the classical Linear Elastic Fracture Mechanics (LEFM) and, second, by a new approach called Linear Elastic Brittle Interface (LEBI) formulation. The material system used is carbon fibre reinforced polymer laminate with epoxy matrix (AS4/8552 Hexcel)* $[0_3/90_3]_S$*. Numerical results show that the LEBI formulation is a useful and efficient tool able to model the transverse and delamination cracks behaviour in* $[0/90]$ *symmetric laminates.*

1. Introduction

Nowadays, some primary structures of commercial aeroplanes are being made of composites. This fact requires a better knowledge of mechanisms of failure in composites. A physically based failure or damage criteria is an essential step towards this objective. All this leads to the necessity of revisiting classical problems of composite laminates such as the mechanism of damage in $[0/90]_S$ laminates [1, 2, 3, 4].

In the present work the linear elastic-brittle interface (LEBI) model developed in Távara *et al.* [5, 6] is used. The linear elastic-brittle constitutive law employed takes into account the variation of the fracture toughness with the fracture mode mixity. The constitutive law also considers the possibility of linear elastic frictionless contact between crack faces, once a portion of the interface is broken. This LEBI model has been implemented in a 2D collocational BEM code.

The present paper is a step forward towards the characterization of the mechanisms of failure of a $[0/90]_S$ laminate. Its aim is to characterize the behaviour of the two types of crack involved in the problem (transverse and delamination) by means of the LEBI formulation, trying to connect predictions with the observed damage of specimens, as shown in [4].

2. Description of the problem

The problem analyzed is shown in Figure 1. It represents a $[0/90]_S$ laminate under tensile loading in the direction of the fibres in the 0° ply, that was solved previously by means of the BEM and using the Virtual Crack Closure Technique (VCCT) to calculate the Energy Release Rate (ERR) by Blázquez *et. al.* [2] and by París *et. al.* [3].

The first damage in this laminate is expected to be the nucleation and growth of cracks in the 90° ply transverse to the load. When one of these cracks approaches the interface with the 0° ply, it is accepted that it stops. New transverse cracks appear in the 90° ply with increasing load until the crack density reaches a critical value. Transverse matrix cracking in 90° ply leads to a load redistribution in the adjacent 0° plies and induces local stress concentrations at the neighborhood of the crack tips that, where the tips are near to the interface, can involve significant interlaminar delamination [3, 7].

For the case analyzed in this work, the material system is a carbon–epoxy (AS4/8552 Hexcel) laminate $[0_3/90_3]_S$: E_{11} = 45.6 GPa, $E_{22} = E_{33}$ = 16.2 GPa, $\nu_{12} = \nu_{13}$ = 0.278, ν_{23} = 0.4, $G_{12} = G_{13}$ = 5.83 GPa, G_{23} = 5.786 GPa, direction 1 being considered the fibre direction. The half-thickness of the 90° plies, t, and the thickness of each of the 0° plies is 0.55 mm. The average separation between transverse cracks is taken to be $2L$ = 4 mm.

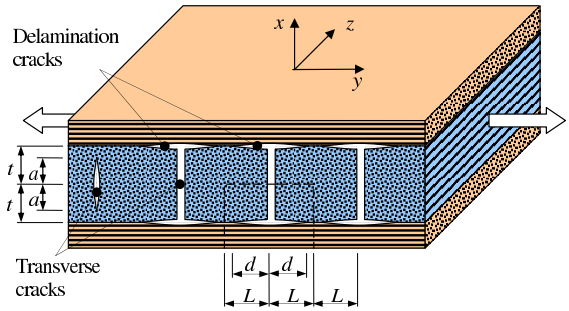

Figure 1. Transverse and delamination cracks in $[0/90]_S$ laminate, taken from [3].

3. Model of the problem

The previously described problem has some usually accepted damage patterns [3], see Figure 2: the first having only a transverse crack, Figure 2(a), the second having a transverse crack that has reached the interface with the 0° lamina, Figure 2(b). The third having a transverse crack that has deflected, starting a symmetric delamination, see Figure 2(c). Finally, the fourth damage pattern, shown in Figure 2(d), indicates that delamination will appear before the transverse crack reaches the interface. This scheme represented in Figure 2(d) is known in Fracture Mechanics as the Cook-Gordon mechanism [8].

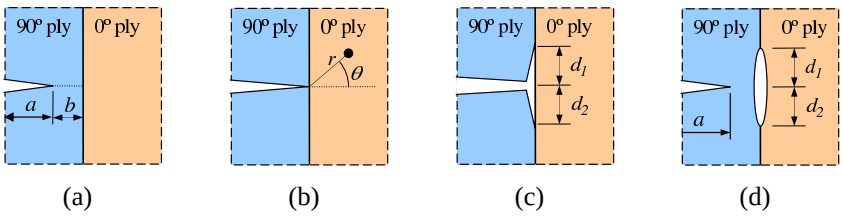

Figure 2. Damage configurations considered with a transverse crack: (a) not reaching the interface, (b) terminated at the interface, (c) deflected at the interface, and (d) approaching a damaged interface (Cook-Gordon mechanism). Slightly modified version of a picture from [3].

As mentioned before, the LEBI model has been used to study the present problem. The cases shown in Figure 2 exhibit symmetry (with respect to the horizontal middle plane in the figure), this fact allows us to study the delamination crack growth either using the configuration shown in Figure 3(a) or (b). Nevertheless, to study the onset and growth of the transverse crack (modeled using the LEBI model), the use of the configuration presented in Figure 3(a) is necessary, since the present BEM code implementation of the interface elements, needs the presence of both solids adjacent to the interface. In the BEM model used to simulate the geometry shown in Figure 3(a) the uniform boundary element mesh has 3860 linear elements, while in the other case (Figure 3(b)) the mesh is formed by 2040 linear elements. In both cases the constant element size is 5μm.

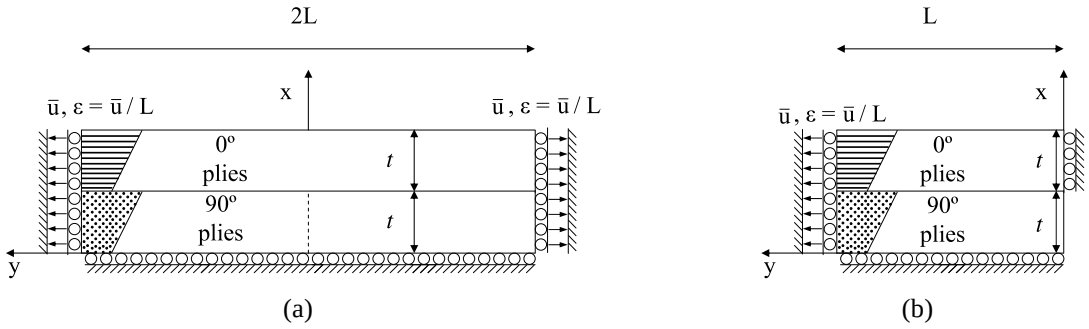

Figure 3. Geometry and boundary conditions for the delamination problem in [0/90] symmetric laminates.

4. Numerical results for transverse and delamination cracks

4.1. Transverse cracks

As mentioned before, to study the onset and growth of the transverse crack, the geometry shown in Figure 3(a) is used. The LEBI elements have been included at the interface between the 0° ply and 90° ply, and also along the assumed crack path of the transverse crack that could appear in the 90° ply (shown in Figure 3(a) with a dashed line).

The properties of the "crack path" at the two positions (transverse or delamination) were considered to be different, see Table 1. Two different combinations were used in order to see the influence of the interface properties in the overall behavior of the problem.

Table 1. Considered combinations of the interface properties in the delamination problem of [0/90] symmetric laminates.

N°	Position	G_{Ic}(Jm^{-2})	$\bar{\sigma}_c$(MPa)	k_n (MPa/μm)	k_t (MPa/μm)
1	transverse	75	61	24.807	8.269
	delamination	75	90	54	18
2	transverse	75	61	24.807	8.269
	delamination	34.454	61	54	18

Notice that in the first combination the fracture toughness in mode I, G_{Ic}, is considered to be the same in both positions, but the critical stress, $\bar{\sigma}_c$, varies leading to different values of the normal stiffness k_n. From Table 1, it can be seen that the ratio of normal and tangential stiffnesses $k_n/k_t = 3$ is defined for all cases considered. In the second combination G_{Ic} values are considered to be different, but having the same value of $\bar{\sigma}_c$.

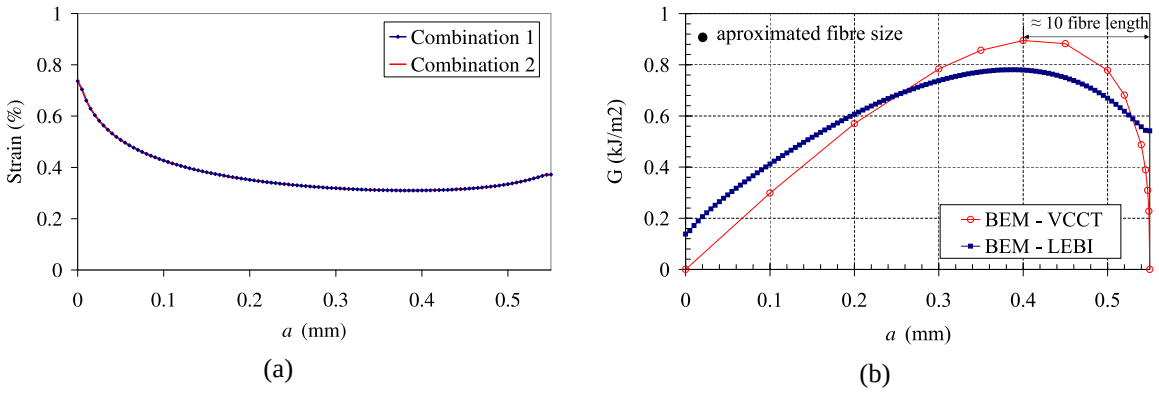

Figure 4. (a) Applied strain versus the length of the transverse crack a. (b) Comparison of the predictions of the ERR (G) obtained by VCCT and the linear elastic-brittle formulation, for a fixed applied strain of 1%.

In Figure 4(a) the actual applied average (longitudinal) strain, $\varepsilon = \bar{u}/L$, versus the length of the transverse crack a is plotted. It can be seen that that once a critical strain is applied the crack grows in an unstable manner (less applied strain is needed) until it reaches the interface between the 0° ply and 90° ply. It should be stressed that in both combinations of interface properties the results are the same. This fact leads to the conclusion that the properties of the interface between the 0° ply and 90° ply ($\bar{\sigma}_c$ and G_{Ic}), has no significant influence on the behavior of the transverse crack, while k_n and k_t values keep the same values for both combinations and the delamination crack has not initiated yet. The fracture energy G_c is always equal to $G_{Ic} = 75\text{Jm}^{-2}$, due to the mode I behavior of the transverse crack and according to Table 1.
In Figure 4(b) the distribution of the values of the ERR of the transverse crack versus the length a, for a fixed applied strain of 1% obtained by means of the VCCT is compared with the results obtained with the LEBI formulation proposed. A reasonable general agreement, from a qualitative point of view can be observed between the obtained results. Nevertheless some differences can also be seen, especially in the zone where the transverse crack has initiated and in the zone just before the transverse crack reaches the interface between 0° and 90° plies . These differences are basically caused because the LEBI model allows an opening and tangential relative displacements at the crack tip and ahead of it, while in the VCCT these relative displacements are zero.

4.2. Delamination cracks

In the following, the onset and growth of the delamination crack is studied. In particular the effects of the consideration or not of an elastic contact algorithm, and the variation of the interface properties, are elucidated.

4.2.1. Contact influence

The delamination crack initiates as open crack and, after a certain crack length size is reached, it starts to be partially closed. Thus, the influence of contact in this specific problem is studied. In one case, once a LEBI element is broken it may enter in frictionless contact according to [6]. In the other case an interpenetration of crack faces is allowed without causing any contact stresses. The properties taken where the ones for Combination 1, see Table 1, and the geometry used is the one shown in Figure 3(b).
In Figure 5(a) a comparison of the actual applied strain versus the length of the delamination

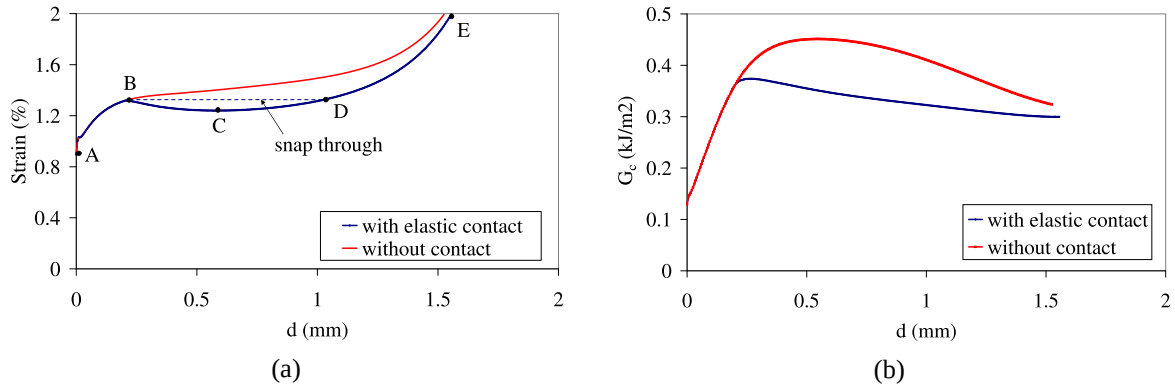

Figure 5. (a) Comparison of the applied strain versus the length of the delamination crack d, considering contact or not. (b) Comparison of the distribution of the fracture toughness necessary to cause the delamination crack growth versus the length d, considering contact or not.

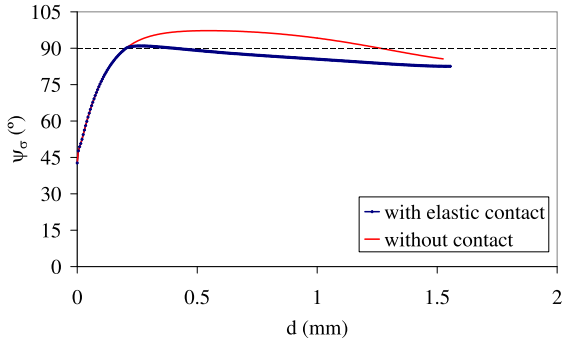

Figure 6. Mixity angle ψ_σ obtained at the crack tip versus the length of the delamination crack d, considering contact or not.

crack d is plotted, considering contact or not. Notice that when contact is considered the delamination crack initially behaves in a stable manner, then a relatively large unstable growth appears where an instability phenomenon called snap-through takes place, and finally a stable growth is reached again. If contact is not considered, allowing overlapping of delamination crack faces, the crack growth is always stable.

Figure 5(b) represents a comparison of the distribution of the fracture energy necessary to cause the crack growth versus the length d. In this case it is noteworthy that when contact is considered the fracture energy necessary to growth is less than when contact is not considered. Thus, frictionless contact makes easier crack propagation. This fact could be explained because of the failure criteria used. As can be seen in [6], when the crack tip is in compression it needs more energy (larger tangential stresses which govern the failure in this problem) to growth. It can also be commented that the differences of the values of the ERR of the delamination crack are almost negligible if contact is considered or not.

Figure 6 represents a comparison of the fracture mode mixity angle ψ_σ ($\tan\psi_\sigma = \tau/\sigma$), obtained at the crack tip, versus the length of the delamination crack d. In a first stage a stable crack growth in mixed mode ($\psi_\sigma \leq 90°$) is observed for two cases. After this stage a great difference of ψ_σ values is obtained. When contact is considered, a small stage of crack growth with the crack tip closed appears, and after this small stage the crack grows in mixed mode again, with the crack tip opened forming a "bubble" near the crack tip. On the other hand, when contact is not considered, the stage of crack growth with the crack tip closed is very large.

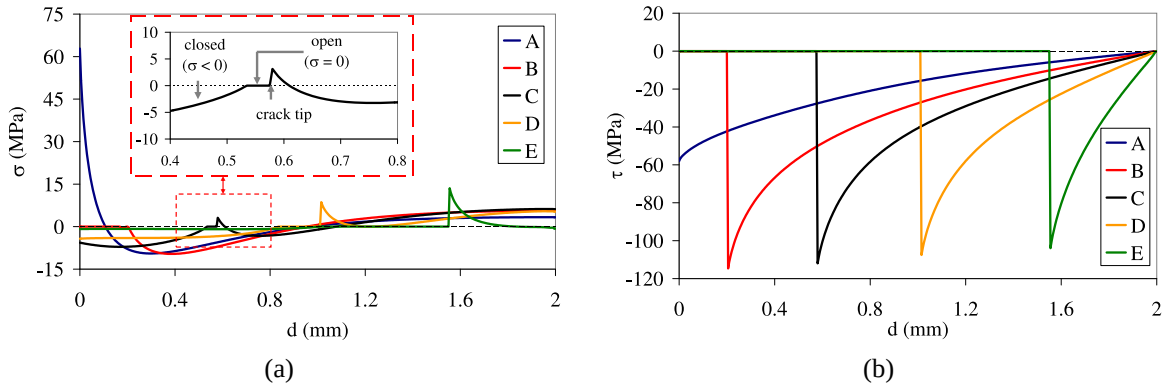

(a) (b)

Figure 7. (a) Normal stresses and (b) tangential stresses obtained at the interface between 0° and 90° plies for the different loads steps shown in Figure 5.

In Figure 7 the normal and tangential stresses at the interface between 0° and 90° plies are plotted for the different load steps shown in Figure 5(a) when elastic contact is considered. As can be seen from these figures the tangential stresses are much larger than the normal stresses during the delamination crack growth. Additionally, in some load steps, a "bubble" formed near the crack tip can be observed ($\sigma = 0$) in Figure 7(a).

4.2.2. Different interface properties

As can be concluded from the previous analysis, the use of contact seems to be relevant for a proper modeling of delamination growth. Thus, taking into account the contact algorithm, the two combinations, according to Table 1, of interface properties are considered in the following. Again the geometry shown in Figure 3(b) is used.

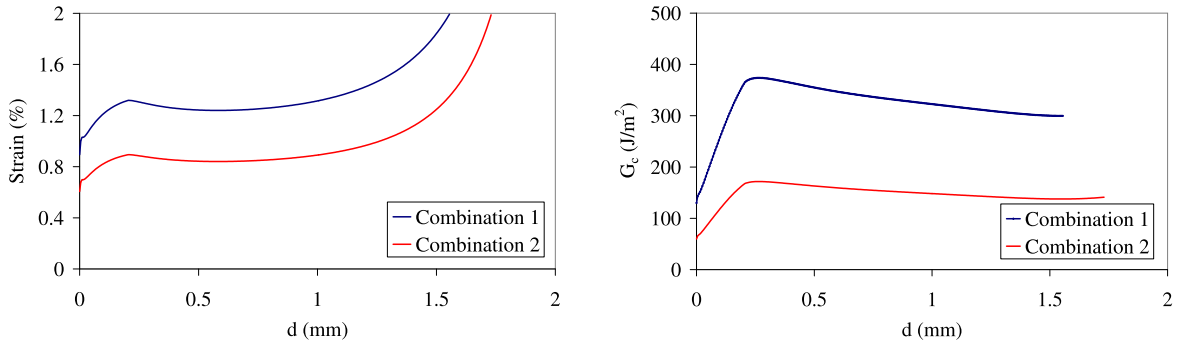

(a) (b)

Figure 8. Comparison of the two combinations considered in Table 1: (a) applied strain versus the length of the delamination crack d, and (b) fracture toughness necessary to cause the crack growth versus the length d.

In Figure 8(a) a comparison of the actual applied strain versus the length of the delamination crack d is plotted, for the two combinations considered in Table 1. Notice that combination 2 with the same applied strain causes a larger delamination crack size. It is also noticeable that both curves are very similar in shape but with very different values, which could be caused because, although $\bar{\sigma_c}$ and G_{Ic} values are different, the values of k_n and k_t are the same in both combinations.

Figure 8(b) represents a comparison of the distribution of the fracture energy necessary to cause

the crack growth versus the length d. As in combination 2 the G_{Ic} associated to the interface is lower, the obtained results are in accordance with this fact. It can be observed that the delamination crack for combination 2 grows easier. It can also be commented that, there are no differences in the values of the ERR of the delamination crack for the two combinations considered in Table 1. Moreover ψ_σ values are exactly the same for both combinations.

4.2.3. Comparison with VCCT results

In a similar way as it was done for transverse cracks, in Figure 9(a) the ERR (G) obtained by O'Brien [9] and McCartney and Blázquez [10], as well as the ERR obtained using the LEBI formulation and the one obtained using VCCT, for a fixed applied strain of 1%, are compared. Notice that LEBI results seem to be in a good qualitative agreement with those obtained by means of the VCCT.

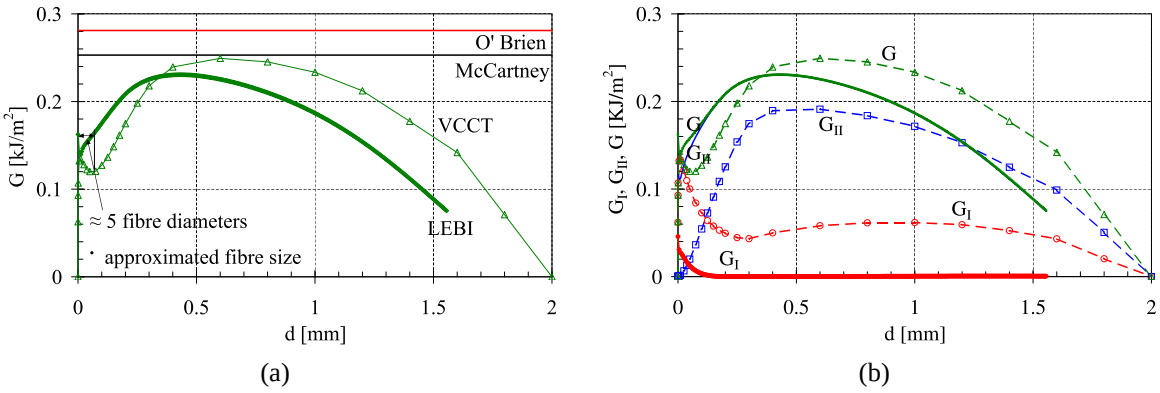

Figure 9. (a) Comparison of the predictions of the ERR (G) for the delamination crack obtained by different authors, VCCT and the linear elastic-brittle interface formulation, for a fixed applied strain of 1%. (b) Comparison of the predictions of the ERR (G) obtained by the VCCT (dashed lines) and the linear elastic-brittle formulation (continuous lines), for a fixed applied strain of 1% versus the length of the delamination crack d.

Finally in Figure 9(b) the ERR components (G_I, G_{II} and G) obtained by the VCCT and the LEBI formulation, for a fixed applied strain of 1% are plotted. Notice that the contribution of mode I and II are in accordance qualitatively by the two methods presented. In fact, it can be said that the larger contribution in mode I obtained by means of the VCCT is caused by the use of a very small value of the virtual crack step length, $\triangle a$. It can be expected that the results obtained by means of the VCCT and a larger value (more realistic) of $\triangle a$ will be in better agreement with the results obtained by means of the present LEBI formulation.

5. Conclusions

As shown by the numerical results presented in this paper, the LEBI formulation seems to be a promising tool to describe the behavior of transverse and delamination cracks in [0/90] symmetric laminates. As shown by the results presented, the BEM tool developed can be considered a useful tool, as crack propagation can be modeled by using always the same uniform mesh. While for the VCCT [2, 3] a refined mesh is necessary near the crack tip, thus for a different load steps, different meshes are needed. It is remarkable that the onset and unstable growth of the transverse crack requires a significatively lower load (applied strain) than the one needed for the onset of the delamination crack. In all the analyzed cases, the transverse crack reached the interface between 0° and 90° plies before the delamination crack onset. Once the delami-

nation crack starts to growth three stages can be clearly identified: (i) initial stage: a relatively short stable growth of the delamination crack takes place with open traction-free crack faces; (ii) intermediate stage: the delamination crack growth becomes unstable and there is contact between the crack faces, except for the zone close to the crack tip where a kind of bubble appears; (iii) final stage: the delamination crack growth becomes stable again. It should be mentioned that, although it was not studied in this paper, the LEBI formulation is capable of reproducing the Cook-Gordon mechanism, see Figure 2(d), by using an adequate combination of interface properties and the properties used for the crack path of the transverse crack.

Acknowledgements
The work was supported by the Junta de Andalucía (Projects of Excellence TEP-1207, TEP 02045 and P08-TEP 04051), the Spanish Ministry of Education and Science through Project TRA2006-08077 and MAT2009 - 140022.

References

[1] A. Blázquez, V. Mantič, F. París, and L. N. McCartney. Stress state characterization of delamination cracks in [0/90] symmetric laminates by BEM. *International Journal of Solids and Structures*, 45:1632–1662, 2008.

[2] A. Blázquez, V. Mantič, F. París, and L. N. McCartney. BEM analysis of damage progress in 0/90 laminates. *Engineering Analysis with Boundary Elements*, 33:762–769, 2009.

[3] F. París, A. Blázquez, L. N. McCartney, and V. Mantič. Characterization and evolution of matrix and interface related damage in $[0/90]_S$ laminates under tension. Part I: Numerical predictions. *Composites Science and Technology*, 70:1168–1175, 2010.

[4] F. París, A. Blázquez, L. N. McCartney, and A. Barroso. Characterization and evolution of matrix and interface related damage in $[0/90]_S$ laminates under tension. Part II: Experimental evidence. *Composites Science and Technology*, 70:1176–1183, 2010.

[5] L. Távara, V. Mantič, E. Graciani, J. Cañas, and F. París. Analysis of a crack in a thin adhesive layer between orthotropic materials. An application to composite interlaminar fracture toughness test. *Computer Modeling in Engineering and Sciences*, 58(3):247–270, 2010.

[6] L. Távara. *Damage initiation and propagation in composite materials. Boundary element analysis using weak interface and cohesive zone models*. PhD Thesis. Universidad de Sevilla: Sevilla, 2010.

[7] JM. Berthelot. Transverse cracking and delamination in cross-ply glass-fiber and carbon-fiber reinforced plastic laminates: static and fatigue loading. *Applied Mechanics Reviews*, 56:111–147, 2003.

[8] J. Cook, J. E. Gordon, C.C. Evans, and D.M. Marsh. A Mechanism for the Control of Crack Propagation in All-Brittle Systems. *Proceedings of the Royal Society of London. Series A, Mathematical and Physical Sciences*, 282:508–520, 1964.

[9] T.K. O'Brien. *Analysis of local delaminations and their influence on composite laminate behavior. In: Delamination and debonding of materials*. ASTM STP 876, Philadelphia, 1984.

[10] L. N. McCartney and A. Blázquez. Delamination model for cross-ply laminates subject to triaxial loading and thermal stresses. *ICCM 17, Edinburgh*, 2009.